

PERTURBATION ANALYSIS OF THE EFFECTIVE EQUATION FOR TWO COUPLED PERIODICALLY DRIVEN OSCILLATORS

ANDRZEJ OKNIŃSKI AND JAN KYZIOŁ

Received 30 November 2005; Revised 13 May 2006; Accepted 21 May 2006

Dynamics of two coupled periodically driven oscillators is analyzed via approximate effective equation of motion. The internal motion is separated off exactly and then approximate equation of motion is derived. Perturbation analysis of the effective equation is used to study the dynamics of the initial dynamical system.

Copyright © 2006 A. Okniński and J. Kyzioł. This is an open access article distributed under the Creative Commons Attribution License, which permits unrestricted use, distribution, and reproduction in any medium, provided the original work is properly cited.

1. Introduction

Coupled oscillators play an important role in many scientific fields, for example, in mechanics, electronics, and biology; see [1, 4] and references therein. In this paper we analyze two coupled oscillators, one of which is driven by an external periodic force. Important example of such a system is a dynamic vibration absorber which consists of a small mass, m_2 , attached to the primary vibrating system of mass m_1 [2, 10]. We make the simplifying approximation that, while the motion of the smaller mass is nonlinear, the motion of the main mass can be treated as linear. Equations describing dynamics of such a system are of the form

$$\begin{aligned}m_1\ddot{x}_1 + \nu_1\dot{x}_1 + \alpha_1x_1 + V(\dot{x}_2 - \dot{x}_1) + R(x_2 - x_1) &= f \cos(\omega t), \\m_2\ddot{x}_2 - V(\dot{x}_2 - \dot{x}_1) - R(x_2 - x_1) &= 0,\end{aligned}\tag{1.1}$$

where α_1 is linear spring constant for a spring connecting mass m_1 with inertial frame of reference, ν_1 is a coefficient of linear damping, V and R represent force of internal friction and elastic restoring force, respectively.

Dynamics of coupled periodically driven oscillators is very complicated [4]. In the recent paper we simplified (1.1) (approximately) reducing it to the Duffing-type effective equation [7, 8]. The effective equation is still very complicated. The main goal of

2 Perturbation analysis of the effective equation

the present paper is to apply perturbation analysis to make progress in understanding dynamics of the effective equation. This, in turn, should clarify dynamics of the exact equation (1.1).

The paper is organized as follows. In Section 2, derivation of the approximate effective equation for internal motion is outlined. Perturbation analysis of the effective equation of motion is described in Section 3 and applied to study stability of nonlinear resonances. In Section 4, computations testing results of the perturbation approach are presented. In Section 5, perspectives of further research are outlined shortly.

2. Derivation of the effective approximate equation for the internal motion

In new variables, $x \equiv x_1$, $y \equiv x_2 - x_1$, (1.1) read

$$\begin{aligned} m\ddot{x} + \nu\dot{x} + \alpha x + V(\dot{y}) + R(y) &= f \cos(\omega t), \\ m_e(\ddot{x} + \ddot{y}) - V(\dot{y}) - R(y) &= 0, \end{aligned} \quad (2.1)$$

where $m \equiv m_1$, $m_e \equiv m_2$, $\nu \equiv \nu_1$, $\alpha \equiv \alpha_1$. Adding (2.1) we obtain an important linear relation between variables x and y :

$$M\ddot{x} + \nu\dot{x} + \alpha x + m_e\ddot{y} = f \cos(\omega t), \quad (2.2)$$

where $M = m + m_e$.

It is possible to separate variables in (2.1) due to its two-body structure to obtain the equation for the internal motion variable y alone. Multiplying the first and the second of (2.1) by m_e and m , respectively, we get

$$mm_e\ddot{x} + m_e\nu\dot{x} + m_eV(\dot{y}) + m_eR(y) = m_e f \cos(\omega t), \quad (2.3a)$$

$$mm_e(\ddot{x} + \ddot{y}) - mV(\dot{y}) - mR(y) = 0. \quad (2.3b)$$

Subtracting (2.3a) from (2.3b) we obtain a new system of equations:

$$M(\mu\ddot{y} - V(\dot{y}) - R(y)) = m_e(\nu\dot{x} + \alpha x - f \cos(\omega t)), \quad (2.4a)$$

$$m_e\ddot{x} = -m_e\ddot{y} + V(\dot{y}) + R(y), \quad (2.4b)$$

where μ is the reduced mass, $\mu = mm_e/(m + m_e)$. Now we can eliminate variable x in (2.4a) differentiating it twice with respect to time and using (2.4b) to obtain the following equations for y :

$$\begin{aligned} \left(M \frac{d^2}{dt^2} + \nu \frac{d}{dt} + \alpha \right) (\mu\ddot{y} - V(\dot{y}) - R(y)) + \varepsilon \left(\nu \frac{d}{dt} + \alpha \right) m_e\ddot{y} &= F \cos(\omega t), \\ m_e\ddot{x} &= -m_e\ddot{y} + V(\dot{y}) + R(y), \end{aligned} \quad (2.5)$$

where $F = m_e \omega^2 f$, $\varepsilon = (m_e - \mu)/m_e = m_e/M$ is a small nondimensional parameter, and (2.4b) was displayed again. Equations (2.5) are equivalent to the initial equations (1.1) [7, 8].

Assuming in (2.5) $0 < \varepsilon \ll 1$ ($m_e \ll M$) and neglecting the term proportional to ε we obtain an approximate effective equation:

$$\mu \ddot{y} - V(\dot{y}) - R(y) = g(t), \quad (2.6a)$$

$$\left(M \frac{d^2}{dt^2} + \nu \frac{d}{dt} + \alpha \right) g(t) = m_e \omega^2 f \cos(\omega t), \quad (2.6b)$$

describing motion of mass m_e with respect to m .

Given the solutions $g(t)$, $y(t)$ of (2.6b), (2.6a) the function $x(t)$ can be determined from the second of (2.5) or (2.2). Let us finally note that it follows from the second of (2.5) that large values of y lead to a large acceleration \ddot{x} of the main mass.

3. Analysis of the approximate effective equation

3.1. Preliminary considerations. Solving (2.6b) we get (see [7, 8])

$$g(t) = Ae^{-\lambda t} \sin(\omega_1 t + \varphi) + B(\omega) \cos(\omega t + \delta), \quad (3.1a)$$

$$\lambda = \frac{\nu}{2M}, \quad \omega_1 = \sqrt{\omega_0^2 - \lambda^2}, \quad \omega_0 = \sqrt{\frac{\alpha}{M}}, \quad (3.1b)$$

$$B(\omega) = \frac{-m_e \omega^2 f}{\sqrt{M^2(\omega^2 - \omega_0^2)^2 + \nu^2 \omega^2}}, \quad \tan(\delta) = \frac{\omega \nu}{M(\omega^2 - \omega_0^2)}. \quad (3.1c)$$

In order to compare the exact equation (2.5) with the approximate equation (2.6) we choose the following forms of functions V , R :

$$V(\dot{y}) = -\nu_e \dot{y}, \quad R(y) = \alpha_e y - \gamma_e y^3, \quad (\nu_e \geq 0, \alpha_e \geq 0, \gamma_e \geq 0) \quad (3.2)$$

so that the Duffing-type effective equation (2.6) is obtained:

$$\mu \ddot{y} + \nu_e \dot{y} - \alpha_e y + \gamma_e y^3 = B(\omega) \cos(\omega t + \delta), \quad (3.3)$$

where λ , $B(\omega)$, and δ are defined in (3.1), and we have neglected the decaying term $Ae^{-\lambda t} \sin(\omega_0 t + \varphi)$ (note that in [7, 8] we have tested effective equation for another form of $R(y)$). Equation (3.3) has three points of equilibrium given by $R(y) = 0$:

$$y_* = 0, \quad y_*^\pm = \pm \sqrt{\frac{\alpha_e}{\gamma_e}}. \quad (3.4)$$

We will refer to a periodic solution encircling only one of the points y_*^\pm as a small orbit (SO) while an orbit encircling all three equilibrium points will be referred to as a large orbit (LO) following [3] (orbits with another geometries are, of course, also possible).

4 Perturbation analysis of the effective equation

3.2. Linear resonances. Linear resonance conditions can be determined for (2.2), (3.3) as well as for (2.6b).

Firstly, if for m_e small enough the term $m_e \ddot{y}$ can be neglected in linear equation (2.2) to yield

$$M\ddot{x} + \nu\dot{x} + \alpha x \cong f \cos(\omega t), \quad (3.5)$$

then the resonance occurs (for small ν) at $\omega \cong \omega_0 = \sqrt{\alpha/M}$. We can thus expect large amplitudes of $x(t)$.

Precisely the same resonance occurs in (2.6b) and the amplitude $B(\omega)$ has (for small ν) a narrow and high maximum around $\omega \cong \omega_0$. In this case $g(t)$ is large in (2.6a) and the solution y reaches large magnitudes as well. Obviously, deeper analysis of (2.6) is however necessary to investigate conditions under which nonlinear resonances can exist. We will perform such analysis in Section 3.3.

Secondly, there is a linear resonance for SO states in the effective equation. Indeed, if we put $y(t) = y_*^\pm + \varepsilon^\pm(t)$, with y_*^\pm given by (3.4), then for small $\varepsilon^\pm(t)$ linear approximation is obtained:

$$\mu \ddot{\varepsilon}^\pm + \nu_e \dot{\varepsilon}^\pm + 2\alpha_e \varepsilon^\pm \cong B(\omega) \cos(\omega t + \delta). \quad (3.6)$$

The resonance condition is thus (for small ν_e) $\omega \cong \tilde{\omega}_0 = \sqrt{2\alpha_e/\mu}$. In this case we can expect that the SO state transforms into LO-type solution. Moreover, it may happen that the two resonance frequencies nearly coincide, $\omega_0 \cong \tilde{\omega}_0$. In such a case for $\omega \cong \omega_0 \cong \tilde{\omega}_0$ the most rapid destabilization of the SO state can be expected.

3.3. Perturbation analysis of nonlinear resonances in the effective equation. We will apply the Krylov-Bogoliubov-Mitropolsky (KBM) perturbation approach [5] to the effective equation (3.3) attempting to find steady-state solutions, working in the spirit of [3, 11] (see also [9]). The effective equation is written as Duffing-type equation:

$$\frac{d^2 y}{dt^2} + h \frac{dy}{dt} - ay + cy^3 = F(\omega) \cos(\omega t), \quad (3.7)$$

where

$$h = \frac{\nu_e}{\mu}, \quad a = \frac{\alpha_e}{\mu}, \quad c = \frac{\gamma_e}{\mu}, \quad F(\omega) = \frac{B(\omega)}{\mu}, \quad (3.8)$$

since for large t the term $Ae^{-\lambda t} \sin(\omega_0 t + \varphi)$ can be neglected (alternatively, we can put this term to zero by the appropriate choice of initial conditions).

Equation (3.7) can be cast into a form suitable for application of the KBM approach:

$$\frac{d^2 y}{dt^2} + \omega^2 y + \varepsilon f(y, \dot{y}, t) = 0, \quad (3.9)$$

with small parameter ε where

$$f(y, \dot{y}, t) = (-\omega_0^2 - a_0 + c_0 y^2)y + h_0 \dot{y} - F_0(\omega) \cos(\omega t), \quad (3.10a)$$

$$\begin{aligned} \omega^2 &= \varepsilon \omega_0^2, & a &= \varepsilon a_0, & c &= \varepsilon c_0, \\ h &= \varepsilon h_0, & F(\omega) &= \varepsilon F_0(\omega). \end{aligned} \quad (3.10b)$$

We will now investigate 1 : 1 nonlinear resonance. The solution is sought in the following form:

$$y(t) = A(t) \cos(\omega t + \varphi(t)) + \varepsilon y_1(t) + \varepsilon^2 y_2(t) + \dots, \quad (3.11)$$

with slowly varying amplitude and phase:

$$\begin{aligned} \frac{dA}{dt} &= \varepsilon M_1(A, \varphi) + \varepsilon^2 M_2(A, \varphi) + \dots, \\ \frac{d\varphi}{dt} &= \varepsilon N_1(A, \varphi) + \varepsilon^2 N_2(A, \varphi) + \dots, \end{aligned} \quad (3.12)$$

and we assume that the series (3.11) converges.

Computing \dot{y} with the help of (3.11), (3.12) and substituting expressions for y, \dot{y} to (3.9), (3.10) and keeping terms of order ε only we get

$$\frac{d^2 y_1}{dt^2} + \omega^2 y_1 = C_1 \cos(\omega t + \varphi) + C_2 \sin(\omega t + \varphi) + D \cos(3\omega t + 3\varphi), \quad (3.13)$$

where

$$\begin{aligned} C_1 &= 2a\omega N_1 + \omega_0^2 A + a_0 A - \frac{3}{4}c_0 A^3 + F_0(\omega) \cos \varphi, \\ C_2 &= 2\omega M_1 + h_0 \omega A + F_0(\omega) \sin \varphi, \\ D &= -\frac{1}{4}c_0 A^3. \end{aligned} \quad (3.14)$$

Equation (3.13) contains resonant terms proportional to C_1, C_2 , referred to as secular terms [5]. Secular terms lead to contributions $\varepsilon y_1(t)$ in (3.11) proportional to $\varepsilon t \cos(\omega t + \varphi)$ and $\varepsilon t \sin(\omega t + \varphi)$ and hence $|\varepsilon y_1(t)|$ grows unboundedly with time. Such contributions invalidate the perturbation expansion (3.11) and are unphysical as well, therefore they have to be excluded [5]. Accordingly, we demand that secular terms vanish, $C_1 = 0, C_2 = 0$, to get

$$\begin{aligned} N_1 &= -\frac{1}{2\varepsilon\omega A} \left(-\omega_0^2 A - a_0 A + \frac{3}{4}c_0 A^3 - F_0 \cos \varphi \right), \\ M_1 &= -\frac{1}{2\varepsilon\omega} (h\omega A + F(\omega) \sin \varphi). \end{aligned} \quad (3.15)$$

6 Perturbation analysis of the effective equation

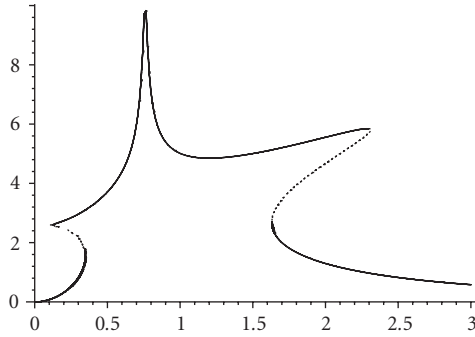


Figure 3.1. Dependence of the amplitude A on the frequency ω . Solid lines denote stable branches while dotted lines mark unstable states.

Since we are seeking a steady-state periodic solution we have to request, according to (3.12) [11],

$$N_1 = M_1 = 0. \quad (3.16)$$

Taking into account (3.15), (3.16), and the definitions (3.10b) we obtain

$$\begin{aligned} A(\omega) \left(\omega^2 + a - \frac{3}{4} c A^2(\omega) \right) + F(\omega) \cos(\varphi(\omega)) &= 0, \\ h\omega A(\omega) + F(\omega) \sin(\varphi(\omega)) &= 0. \end{aligned} \quad (3.17)$$

Finally, solving (3.17) we get conditions for the amplitude and the phase shift:

$$\begin{aligned} A(\omega) &= \frac{F(\omega)}{\sqrt{(h\omega)^2 + (\omega^2 + a - (3/4)cA^2(\omega))^2}}, \\ \tan \varphi(\omega) &= \frac{h\omega}{\omega^2 + a - (3/4)cA^2(\omega)}, \end{aligned} \quad (3.18)$$

and equations for the correction $y_1(t)$:

$$\begin{aligned} \frac{d^2 y_1}{dt^2} + \omega^2 y_1 &= -\frac{1}{4} c_0 A^3(\omega) \cos(3\omega t + 3\varphi), \\ y_1(t) &= \frac{1}{32\omega^2} c_0 A^3(\omega) \cos(3\omega t + 3\varphi). \end{aligned} \quad (3.19)$$

Solving (3.18) for the following values of parameters $m = 1$, $m_e = 0.04$, $\nu = 0.024$, $\nu_e = 0.018$, $\alpha = 0.6$, $\alpha_e = 0.05$, $\gamma_e = 0.01$, $f = 5.5$ (all parameter values are in the SI units), for example, we obtain the typical form of the graph $A(\omega)$ in Figure 3.1.

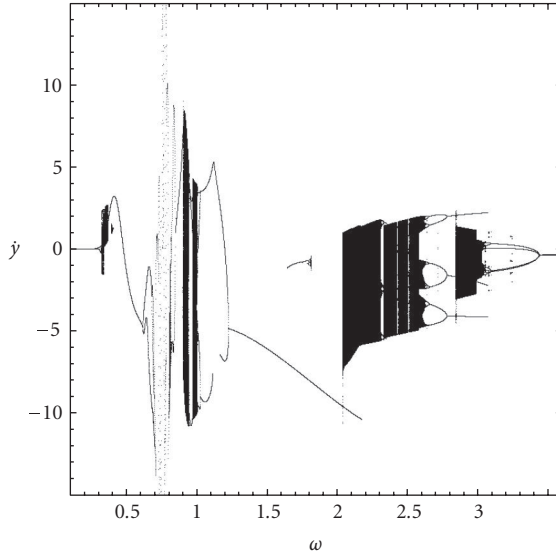


Figure 4.1. Bifurcation diagram for the effective equation.

Stability of the solution (3.18) is investigated considering the perturbed solution, $A + \delta A$, $\varphi + \delta\varphi$. We get from (3.12)

$$\begin{aligned} \frac{d}{dt} \delta A &= \varepsilon \left(\frac{\partial M_1}{\partial A} \delta A + \frac{\partial M_1}{\partial \varphi} \delta \varphi \right), \\ \frac{d \delta \varphi}{dt} &= \varepsilon \left(\frac{\partial N_1}{\partial A} \delta A + \frac{\partial N_1}{\partial \varphi} \delta \varphi \right), \end{aligned} \quad (3.20)$$

where only terms linear in ε were kept. Substituting in (3.20) $\delta A = A_0 e^{\lambda t}$, $\delta \varphi = \varphi_0 e^{\lambda t}$ we obtain eigenequation for A_0 , φ_0 , and λ . The condition of stability of solution (3.18) is equivalent to $\text{Im}(\lambda) < 0$. We have performed such simple stability analysis for values of the parameters given above. Stable and unstable branches have been shown in Figure 3.1.

4. Computational results

We have performed computations for the functions V , R chosen in form (3.2). In Figures 4.1, 4.2, results of computations are shown for the effective and the exact equations, respectively. We have computed bifurcation diagrams running the program DYNAMICS [6]. The program integrated these equations using the fourth-order Runge-Kutta method with a fixed but ω -dependent step size $h(\omega)$ of the independent variable t . The bifurcation diagrams show the projection of the attractors in the Poincaré section, $t = \text{const}$, onto the coordinate \dot{y} for a given value of the control parameter ω . This choice of the Poincaré section is motivated by the symmetry of the system, $t \rightarrow t + T(\omega)$, $T(\omega) = 2\pi/\omega$

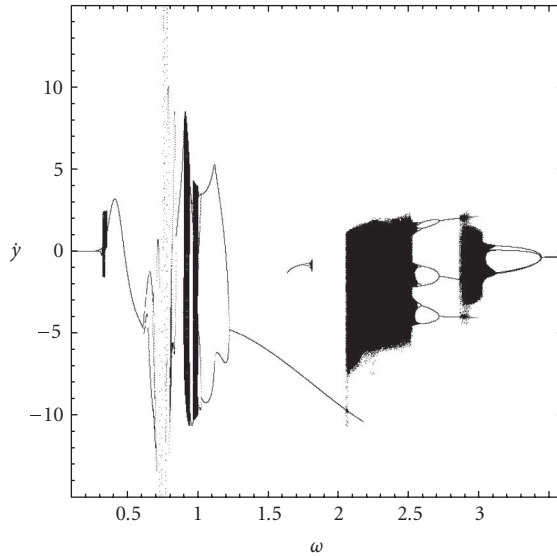


Figure 4.2. Bifurcation diagram for the exact equation.

[4]. The time interval $[0, T(\omega)]$ was divided into N subintervals and hence the step size was selected as $h(\omega) = T(\omega)/N$, with $N = 1024$. This procedure preserved the exact symmetry $t \rightarrow t + T(\omega)$.

The computations were performed for the parameter values given in the preceding section and variable ω . First of all, we realize that the bifurcation diagrams in Figures 4.1, 4.2 for the effective and exact equations are similar. In both figures large amplitudes of relative motion of the small mass are present for $\omega \cong \omega_0 = \sqrt{\alpha/M} = 0.76$, that is, when $B(\omega)$ is large (or, equivalently, near the resonance frequency of (2.2)).

In Figures 4.1, 4.2 SO states can be seen for $\omega > 2.8$, 1 : 3 nonlinear resonance appears for $\omega < 3.05$, and 1 : 1 nonlinear resonance is present for $1.2 < \omega < 2.2$ (the branch with large amplitudes of \dot{y}), $1.6 < \omega$ (the branch with small amplitudes of \dot{y}) and $\omega \approx 0.4$.

We will analyze shortly the 1 : 1 resonance comparing Figures 4.1 and 3.1. The first branch of this resonance ends at $\omega \approx 2.2$ (but for specially chosen initial condition it can be continued up to $\omega \cong 2.3$) in agreement with plot of $A(\omega)$, Figure 3.1. The second branch starts at $\omega > 1.64$ (but for carefully chosen initial conditions it can be continued down to $\omega \approx 1.6$) again in agreement with plot of $A(\omega)$, Figure 3.1, where the lower branch starts at $\omega = 1.60$. It turns out that at lower branch for $\omega > 1.6$ LO states are at first present which for $\omega \gtrsim 1.7$ transform into SO states. This phenomenon can be easily understood if we recall possibility of SO resonance occurring at $\omega \cong \tilde{\omega}_0 = \sqrt{2\alpha_e/\mu} = 1.61$. It follows that near the resonance frequency SO states cannot exist and LO states are created. Since the lower branch of $A(\omega)$ is a decreasing function of ω the LO states cannot be stable too far from the resonance at $\omega = \tilde{\omega}_0$ and thus they transform into SO states. Analogous dynamical phenomena are present in the exact system; cf. Figure 4.2.

Let us note finally that in Figures 4.1, 4.2 transient phenomena are visible as it is suggested by presence of the decaying term $Ae^{-\lambda t} \sin(\omega_1 t + \varphi)$ in the function $g(t)$; cf. (2.6a), (3.1a).

5. Summary and discussion

Our analytical as well as numerical results cast light on the dynamics of nonlinear dynamic vibration absorber described by (1.1) or (2.1) and on the approximate effective equation (2.6). Let us first notice that our approximations lead to the effective equation describing relative motion of a smaller mass with respect to the main mass; cf. (2.6), that is valid for arbitrary form of nonlinear forces $V(\dot{y})$, $R(y)$ and sufficiently small $\varepsilon = m_e/M$ (the motion of the main mass can be obtained from (2.4b)). In the case of our computations with $\varepsilon = 0.04$ and $V(\dot{y})$, $R(y)$ given by (3.2) the bifurcation diagrams computed for the exact system (2.1) and the approximate one (2.6); cf. Figures 4.1, 4.2 that are indeed very similar (see also [8] for other forms of $V(\dot{y})$, $R(y)$).

Analysis of (2.6), (3.1a) suggests that for small values of linear damping constant ν presence of transition states can be expected in dynamics of the effective equation due to the term $Ae^{-\lambda t} \sin(\omega_1 t + \varphi)$, and, for small ε , in dynamics of the exact equation. Indeed, long transients were observed for both equations; see Figures 4.1, 4.2, and [8].

It follows from Sections 3.1, 3.2 that there is always a resonance in the effective equation (2.6) (for small ν) at $\omega \cong \omega_0 = \sqrt{\alpha/M}$; see (3.1a). In this case $g(t)$ is large in (2.6a) and the solution y reaches large magnitudes as well. Indeed, we can see vibrations with high amplitudes near $\omega \cong \sqrt{\alpha/M} = 0.76$ in Figures 4.1, 4.2. Motivated by this result we have performed analysis of 1 : 1 nonlinear resonance for the effective equation (3.3) in Section 3.3. We have determined, using the Krylov-Bogoliubov-Mitropolsky perturbation approach, the dependence of the amplitude A of the resonance on the frequency ω . It follows from Figure 3.1 that the graph $A(\omega)$ has a high but a narrow maximum near $\omega \cong \sqrt{\alpha/M}$ and the stable branch of high amplitude resonance ends, for growing ω , at $\omega \cong 2.3$. These results agree well with computational results presented in Figures 4.1, 4.2. The stable branch in both figures ends at $\omega \approx 2.2$, but for specially chosen initial condition it can be continued up to $\omega \cong 2.3$, in agreement with plot of $A(\omega)$, Figure 3.1.

Let us remark finally, that it is possible to carry out the investigations further applying perturbation analysis directly to the first of the exact equations (2.5) since it contains the small parameter $\varepsilon = m_e/(m_e + m) < 1$.

References

- [1] J. Awrejcewicz, *Bifurcation and Chaos in Coupled Oscillators*, World Scientific, New Jersey, 1991.
- [2] J. P. Den Hartog, *Mechanical Vibrations*, 4th ed., Dover, New York, 1985.
- [3] K. L. Janicki and W. Szemplińska-Stupnicka, *Subharmonic resonances and criteria for escape and chaos in a driven oscillator*, Journal of Sound and Vibration **180** (1995), no. 2, 253–269.
- [4] J. Kozłowski, U. Parlitz, and W. Lauterborn, *Bifurcation analysis of two coupled periodically driven Duffing oscillators*, Physical Review E **51** (1995), no. 3, 1861–1867.
- [5] A. H. Nayfeh, *Introduction to Perturbation Techniques*, John Wiley & Sons, New York, 1981.
- [6] H. E. Nusse and J. A. Yorke, *Dynamics: Numerical Explorations*, Applied Mathematical Sciences, vol. 101, Springer, New York, 1994.

10 Perturbation analysis of the effective equation

- [7] A. Okniński and J. Kyzioł, *Analysis of two coupled periodically driven oscillators via effective equation of motion*, Proceedings of 7th Conference on Dynamical Systems, Theory and Applications, vol. 2, Łódź, December 2003, pp. 639–644.
- [8] ———, *Analysis of two coupled periodically driven oscillators via effective equation of motion*, Machine Dynamics Problems **29** (2005), no. 2, 107–114.
- [9] J. Osiecki, lecture notes, to be published.
- [10] S. S. Oueini, A. H. Nayfeh, and J. R. Pratt, *A review of development and implementation of an active nonlinear vibration absorber*, Archive of Applied Mechanics **69** (1999), no. 8, 585–620.
- [11] W. Szemplińska-Stupnicka, *The Behavior of Non-Linear Vibrating Systems*, Kluwer Academic, Massachusetts, 1990.

Andrzej Okniński: Physics Division, Kielce University of Technology, Al. 1000-lecia PP 7,
25-314 Kielce, Poland
E-mail address: fizao@tu.kielce.pl

Jan Kyzioł: Physics Division, Kielce University of Technology, Al. 1000-lecia PP 7,
25-314 Kielce, Poland
E-mail address: j.kyziol@wp.pl